Bicyclic proline analogues as organocatalysts for stereoselective aldol reactions: an *in silico* DFT study†

C. B. Shinisha and Raghavan B. Sunoj*

Received 5th February 2007, Accepted 28th February 2007
First published as an Advance Article on the web 20th March 2007
DOI: 10.1039/b701688c

Density functional theory has been employed in investigating the efficiency of a series of bicyclic analogues of proline as stereoselective organocatalysts for the aldol reaction. Three classes of conformationally restricted proline analogues, as part of either a [2.2.1] or [2.1.1] bicyclic framework, have been studied. Transition states for the stereoselective C–C bond formation between enamines derived from [2.2.1] and [2.1.1] bicyclic amino acids and *p*-nitrobenzaldehyde, leading to enantiomeric products, have been identified. Analysis of the transition state geometries revealed that the structural rigidity of catalysts, improved transition state organization as well as other weak interactions influence the relative stabilities of diastereomeric transition states and help contribute to the overall stereoselectivity in the aldol reaction. These bicyclic catalysts are predicted to be substantially more effective in improving the enantiomeric excess than the widely used organocatalyst proline. Enantiomeric excesses in the range 82–95% are predicted for these bicyclic catalysts when a sterically unbiased substrate such as *p*-nitrobenzaldehyde is employed for the asymmetric aldol reaction. More interestingly, introduction of substituents, as simple as a methyl group, at the *ortho* position of the aryl aldehyde bring about an increase in the enantiomeric excess to values greater than 98%. The reasons behind the vital energy separation between diastereomeric transition states has been rationalized with the help of a number of weak interactions such as intramolecular hydrogen bonding and Coulombic interactions operating on the transition states. These predictions could have wider implications for the rational design of improved organocatalysts for stereoselective carbon–carbon bond-forming reactions.

Introduction

The search for metal-free organocatalysts has been in the forefront of research in organic chemistry in recent years.[1] Proline has evolved as a prototypical example of an organocatalyst with capabilities for a diverse range of asymmetric transformations.[2] The last couple of years have witnessed increasing activities toward identifying improved proline analogues as well as other organocatalysts for asymmetric catalysis.[3] Both theoretical and experimental studies have been reported that propose proline analogues capable of catalyzing stereoselective aldol reactions.[4] The synergy between experimental and theoretical studies has contributed to the evaluation of the mechanism of proline-catalyzed asymmetric reactions.[5]

In one of the earliest examples, reported more than three decades ago, namely the Hajos–Parrish–Eder–Sauer–Wiechert reaction, proline was found to be effective in catalyzing the intramolecular asymmetric cyclodehydration of an achiral ketone to the unsaturated Wieland–Miescher ketone.[6] Whereas a number of mechanisms were initially considered for this reaction, the one involving two molecules of proline in the catalytic process, proposed by Agami *et al.*, received early acceptance.[7] Recently, Houk and co-workers have examined the involvement of different mechanisms for this reaction using density functional theory (DFT) methods.[8,9] A number of possible transition states for the key C–C bond formation step, which determines the stereochemistry of the reaction, has been proposed. A carboxylic acid assisted enamine mechanism involving only one proline molecule was found to be favourable. In fact, this mechanism, originally proposed by Jung,[10] was overlooked due to the widespread acceptance of Agami's mechanism. The single-proline-catalyzed mechanism for aldol reactions was subsequently re-examined by Houk, List and co-workers with the help of more accurate experimental methods.[11] Proline-catalyzed aldol reactions showed a first-order kinetic dependence on the catalyst concentration, and also exhibited a linear relationship between the enantiomeric excess of proline and that of the product.[3a,11] Thus, the latest experimental results, in concert with DFT studies, support the single-proline-catalyzed mechanism for aldol reactions.

Computational investigations have been used both in conjunction with experimental studies and independently to gaining insights into stereoselective organic reactions. The concurrence between the predicted and experimentally determined enantiomeric excess has generally been quite impressive. Some such examples include the studies on proline-catalyzed aminoxylations,[12] Mannich reactions,[5b] and α-alkylations.[5d,e] DFT calculations, in particular those using the B3LYP functional,[13] have been effectively employed in probing the differential interactions in diastereomeric

Department of Chemistry, Indian Institute of Technology Bombay, Powai, Mumbai, 400076, India. E-mail: sunoj@chem.iitb.ac.in; Fax: +91 22-2572-3480 or +91 22-2576-7152

† Electronic supplementary information (ESI) available: Total electronic energies, optimized coordinates and single-point energies of all structures reported in the text, Fig. S1–S5, Tables S1–S10 and full list of citations for Gaussian 98 and Gaussian 03 (ref. 47 in the text). See DOI: 10.1039/b701688c

TSs that contribute to the vital energy differences responsible for enantioselectivity in these reactions.[14] Through their studies on the proline-catalyzed asymmetric aldol reaction, Houk and co-workers have demonstrated that enantiomeric excesses predicted using the B3LYP transition state calculations are in remarkable agreement with those obtained experimentally.[15] Weak hydrogen bonding as well as other electrostatic interactions are reported to be crucial in stabilizing the transition states.[1d,16]

Mechanistic investigations into the proline-catalyzed direct aldol reaction between ketones and aldehydes using DFT have been reported previously.[17] The stereoselectivity has been identified as being controlled by the crucial C–C bond formation step, which involves the nucleophilic addition of the enamine to the electrophilic aldehyde and concomitant proton transfer from the carboxylic acid group to the developing alkoxide ion (Scheme 1).[15a,18] Finally, hydrolysis of the resulting adduct, with defined stereochemistry, furnishes the desired β-hydroxy ketone as the product.

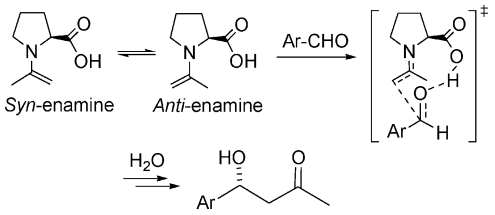

Scheme 1 Addition of enamines to the electrophilic aldehyde in the selectivity-determining step.

The prochiral faces of the electrophile and the *syn* and *anti* conformations of the enamine could give rise to four different stereochemical modes of approach between the reactants. Additionally, a number of possible TSs with varying dihedral angles between the substituents around the incipient C–C bond can also be envisaged. The lower energy TSs have been suggested to possess intramolecular hydrogen bonding between the developing alkoxide ion and the carboxylic acid group.[15a] The product ratio and the enantiomeric excess calculated using such lower energy TSs was found to be in good agreement with experimental observation. In particular, the computed enantiomeric excess using the gas-phase enthalpy of activation ($\Delta H^{\dagger}_{298\,K}$) was found to be in close agreement with the experimental results. Furthermore, the activation enthalpies have shown minimum error with respect to the experimentally determined kinetic parameters.[19]

DFT methods have been successfully applied to gain better insights on reaction mechanisms as well as towards rationalizing experimental stereoselectivity in a number of cases other than those described above.[20] We believe that the predictive potential of theoretical models can be further exploited in accelerating this burgeoning area of chemical research. From a slightly different perspective, one can identify an underlying parallelism between the virtual screening protocols adopted in rational drug design and our DFT-based approach to designing new organocatalysts described in the present context. Computer-aided methods using scoring functions and related parameters have significantly contributed to drug discovery, as well as to organic chemistry.[21] In the present thesis, we intend to convey the use of quantum chemical calculations as a virtual screening tool for designing improved organocatalysts.

Among the increasing number of proline analogues reported as potential organocatalysts, the major changes include conversion/replacement of the carboxylic acid group as well as elaborations at the β and γ positions.[22] All such attempts thus far have revolved around monocyclic proline analogues, except for couple of reports on 4,5-methanoprolines.[4b,23] The pyrrolidine ring conformation in proline is believed to be important in chirality transfer,[8] which could play a vital role in organizing the transition state that is formed between the substrate and catalyst along the most enantioselective path.[1c] The pyrrolidine ring is also known to be better suited to aldol reactions than other cyclic secondary amines such as pipecolic acid and 2-azetidinecarboxylic acid.[3a] Primary amino acids have also been studied as catalysts for aldol reactions, but good enantiomeric excesses were observed only when the substrates employed were cyclic ketones with reduced conformational flexibility.[24]

Proline can exist in different interconvertible conformations by virtue of the puckered pyrrolidine ring.[25] Therefore, it is logical to anticipate that restricting the conformational freedom of the pyrrolidine ring could have a direct impact on the stereoselectivity of reactions. Greater rigidity of the catalyst could impart improved stability and organization of the transition states, and help keep the entropy loss to a relatively minimal level. Moreover, detailed knowledge on the controlling elements such as structure, conformation and energetics of catalyst, substrate and transitions states will be very valuable towards designing improved catalysts.[1d,26]

We reasoned that introducing geometrical constrains on the catalyst can lead to relatively ordered transition states capable of influencing the stereochemical outcome of the reaction. One of the broader objectives at this juncture is to propose how a standard stereoselective aldol reaction can benefit from complete modeling of the reaction and by close inspection of the selectivity-determining transition state. In the present investigation, we have designed a series of novel bicyclic-bifunctional analogues of proline. These catalysts are evaluated for their ability to promote the stereoselective aldol reaction between acetone and *p*-nitrobenzaldehyde (Scheme 2), using DFT methods.

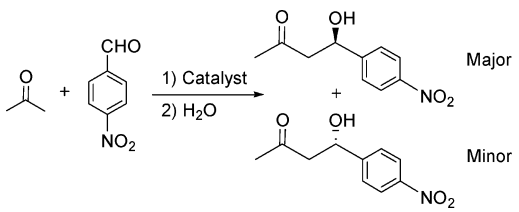

Scheme 2 General scheme of the model aldol reaction investigated in the present work.

Results and discussion

As described above, the mechanism of the organocatalyzed aldol reaction has been proposed to proceed through an enamine intermediate. In this study, we have entirely focused on the selectivity-controlling C–C bond formation step in the aldol reaction between acetone and *p*-nitrobenzaldehyde. This step involves the attack of the enamine formed between acetone and the catalyst (a secondary amine) on the electrophilic aldehyde. Since the aldehyde offers two prochiral faces, the stereoselectivity of the overall reaction will be

critically dependent on this step. In the present study, *re* and *si* facial attack on *p*-nitrobenzaldehye by *anti*- and *syn*-enamines are investigated. The TSs corresponding to attack of the *anti*-enamine on the *re* and *si* faces of the aldehyde are respectively denoted as a-*re* and a-*si*, and that of the *syn*-enamine are referred to as s-*re* and s-*si*. These stereochemical modes of addition are depicted in Scheme 3. The relative energies between the diastereomeric TSs are then calculated, in order to obtain the kinetic preference for the formation of one enantiomer over the other. This energy difference is then translated into enantiomeric excess (ee) using the absolute rate theory.[15a]

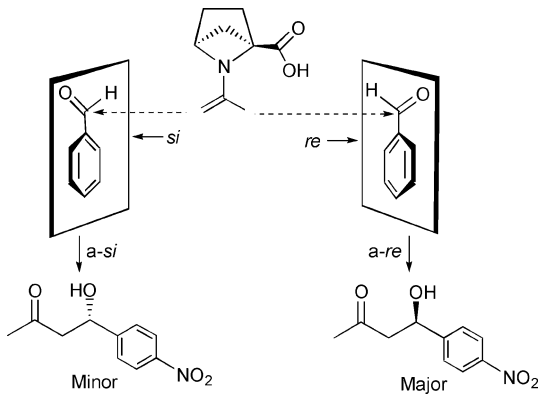

Scheme 3 Different possible stereochemical modes of addition for the *anti*-enamine (derived from catalyst **3** and acetone) with benzaldehyde.

The catalytic ability of bifunctional amino acids, when tailored onto a rigid bicyclic framework, in the aldol reaction is studied in detail below. We have considered three important conformations of proline contained within a bicyclic framework (Scheme 4). The first set has an envelope conformation in which the -NH is out-of-plane in a [2.2.1] or [2.1.1] bicyclic system and its various analogues (**1–7**). In the second set (**8**), C-7 heads the envelope conformation of the proline skeleton. In the third set, the conformation of proline has been constrained as part of a [2.2.1] or [2.1.1] bicyclic system (**9**, **10**). Additionally, a [2.1.1] bicyclic system having a 1,3-relationship between the amino and the carboxylic acid groups (**11**) is also investigated. Interestingly, the synthesis and other applications of a few of these proposed azabicyclic compounds

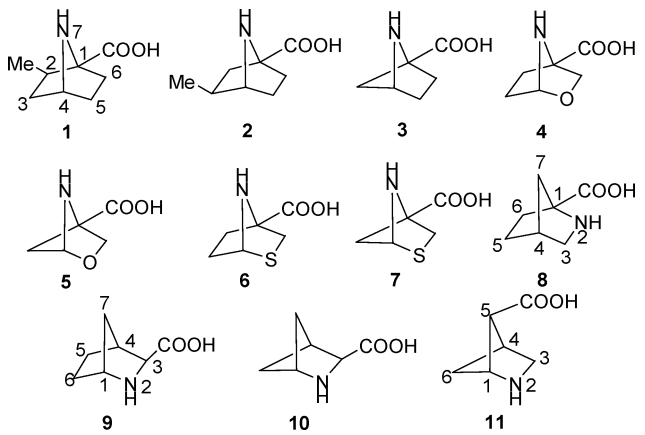

Scheme 4 Bicyclic bifunctional asymmetric catalysts for the stereoselective aldol reaction.

are known.[27] Some of these azabicyclics have been reported to be useful as peptidomimetics, since they are capable of inducing conformational changes in peptides, which could be useful in studying receptor recognition.[28]

The pyrrolidine envelope conformer with an out-of-plane -NH group, when contained within a bicyclic framework as in **1** and **2**, will apparently lose its inherent chirality due a plane of symmetry. While restricted conformers, such as that in a [2.2.1] bicyclic system, could have significant nitrogen inversion barriers ($\Delta G_{expt} = 13.77$ kcal mol^{-1}), the molecule will be achiral under most practical conditions.[29] Such a high barrier probably arises due to the repulsion between nitrogen lone pairs and bonding electrons on the two carbon–carbon bridges and the lack of flexibility at the C–N–C bond angle. To impart inherent chirality to these catalysts and also as an early step towards investigating the effect of substituents, we introduced methyl groups at suitable positions on the bicyclic system, as shown in Scheme 4 (**1** and **2**). The azanorbornyl systems bearing a nitrogen at the 7-position (see the numbering for compound **1**, Scheme 4) are known to be highly pyramidal around the nitrogen atom.[30] The orientation of the carboxylic acid group at the bridge-head position is therefore expected to be restricted due to the intramolecular hydrogen bonding with the amino nitrogen.[31] Another logical extension at this juncture is to restrict the amino group to an out-of-plane position with the help of a methylene bridge, as in a [2.1.1] bicyclic system. This will result in catalyst **3**. The predicted enantiomeric excesses for the asymmetric aldol reactions obtained using these bicyclic catalysts, along with the underlying factors responsible for the stereoselectivity, are summarized below.

As described earlier, the stereoselectivity is controlled by the addition of enamines to the electrophile. We have therefore considered two important enamine conformations as a starting point. On the basis of the computed energies, the lowest energy conformer of the enamine derived from different catalysts could either be *syn* or *anti* with respect to the carboxylic acid group. The *syn*-enamines formed from catalysts **1–7** are found to be more stable than the *anti*-enamines.[32] More importantly, the TSs for the addition of enamines to aldehydes are found to be energetically more favourable for the *syn*-enamines than for the corresponding *anti*-enamines. As a representative example, optimized TS geometries for four possible addition modes of enamine **1** to *p*-nitrobenzaldehyde are provided in Fig. 1.

When the enamine adds to the aldehydic group, the developing alkoxide ion tends to abstract the proton from the carboxylic acid group (Scheme 1). The analysis of the TSs revealed that the geometry for such proton transfer is optimal for TSs involving the *syn*-enamine.[33] Further, the geometric distortion suffered by the resulting iminium ion in the case of the *syn*-enamines is found to be minimal when compared with an ideal planar geometry around the nitrogen atom, exhibiting closer resemblance with the product geometry. These factors would undoubtedly contribute toward improved stabilization for the *syn*-enamine TSs. The planarity of the putative iminium moiety for each TS is analyzed in detail using the C_{ring}–N–C–$C_{iminium}$ dihedral angles, described as θ_1– θ_4 (inset, Fig. 1).[34] Interesting correlations between the activation barriers and these dihedral angles emerge when different TSs are compared. Larger deviations from planarity are generally found for additions involving higher activation barriers. For instance, the θ_1 and θ_3 values in the lower-barrier s-*re* and s-*si* TSs for

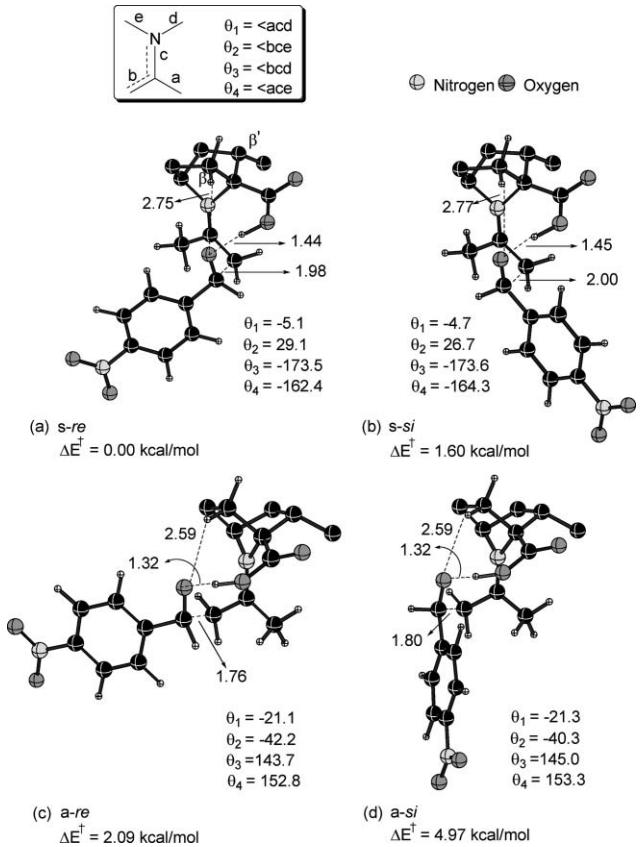

Fig. 1 The B3LYP/6-31G*-optimized transition state geometries for four unique stereochemical modes of addition for enamines derived from catalyst **1** to *p*-nitrobenzaldehyde. Only selected hydrogens on the catalyst are shown for clarity. Activation barriers $\Delta E^{\dagger}$ were obtained at the CPCM/B3LYP/6-311+G**//B3LYP/6-31G* level using DMSO as the solvent. Angles are given in degrees and distances in Å.

catalyst **1** imply a nearly planar geometry around the iminium nitrogen. The deviation for the *syn*-enamine additions are found to be only about ±5°, whereas the corresponding values for the a-*re* and a-*si* TSs are of the order of ±35°, indicating a larger geometric distortion for the developing iminium ion. Such deviations lead to reduced electrostatic stabilization in the TSs and perhaps result in higher activation barriers for *anti*-enamine additions than for *syn*-enamines. Interestingly, the differences in activation barriers between the *syn*- and *anti*-enamine additions are much more pronounced in [2.1.1] bicyclic catalysts (**3**, **5** and **7**) than in [2.2.1] bicyclic systems. It may be noticed that the rigidity of the [2.1.1] bicyclic framework leads to a less favourable proton transfer from the carboxylic acid group to the developing alkoxide in the *anti*-enamine TSs. Such a proton transfer is facilitated at the expense of greater geometric distortion around the developing iminium nitrogen.[35] Another contributing factor helping to achieve additional stabilization for the s-*re* TSs presumably originates from the C–H···π stabilizing interaction between the CH_3-hydrogens of the enamine/iminium with the aryl group of the aldehyde (Fig. 1a).[36] Other stereoisomeric TSs involved in this example (*i.e.*, s-*si* as well as a-*re*/a-*si* TSs) lack such interactions. The relative activation barriers would eventually depend on the presence or absence of all these stabilizing interactions. The relative activation enthalpies calculated based on

Table 1 Computed activation barriers ($\Delta E^{\dagger}$) obtained at the $CPCM_{(DMSO)}$/B3LYP/6-311+G**//B3LYP/6-31G* level for the addition of enamines to *p*-nitrobenzaldehyde, and the corresponding enantiomeric excess for catalysts **1** to **7**[a]

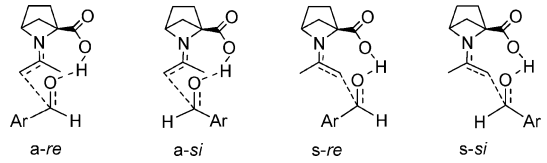

Catalyst	Mode of approach	$\Delta E^{\dagger}$/kcal mol^{-1} [b] Absolute	Relative	ee (%)
1	a-*re*	4.52 (6.77)	2.09 (2.20)	87 (87)
	a-*si*	7.40 (9.59)	4.97 (5.02)	
	s-*re*	4.13 (6.16)	0.00 (0.00)	
	s-*si*	5.73 (7.75)	1.60 (1.58)	
2	a-*re*	0.59 (3.95)	2.38 (2.84)	85 (85)
	a-*si*	3.56 (6.79)	5.35 (5.69)	
	s-*re*	4.93 (6.69)	0.00 (0.00)	
	s-*si*	6.43 (8.21)	1.50 (1.52)	
3	a-*re*	12.22 (15.35)	13.04 (14.57)	82 (87)
	a-*si*	15.28 (18.25)	16.11 (15.86)	
	s-*re*	0.59 (6.29)	0.00 (0.00)	
	s-*si*	1.96 (7.89)	1.37 (1.60)	
4	a-*re*	8.26 (10.47)	3.75 (4.02)	91 (92)
	a-*si*	11.22 (17.24)	6.72 (10.79)	
	s-*re*	7.16 (8.94)	0.00 (0.00)	
	s-*si*	8.99(10.87)	1.82 (1.93)	
5	a-*re*	12.15 (15.69)	13.31 (14.28)	92 (89)
	a-*si*	31.32 (2.21)	32.48 (2.91)	
	s-*re*	3.25 (6.71)	0.00 (0.00)	
	s-*si*	5.18 (8.43)	1.93 (1.72)	
6	a-*re*	22.91 (25.75)	20.59 (20.52)	90 (91)
	a-*si*	10.17 (13.30)	7.85 (8.08)	
	s-*re*	11.02 (8.06)	0.00 (0.00)	
	s-*si*	12.81 (9.88)	1.79 (1.81)	
7	a-*re*	21.66 (22.33)	16.10 (16.24)	84 (85)
	a-*si*	24.87 (25.43)	19.31 (19.34)	
	s-*re*	−0.97 (1.16)	0.00 (0.00)	
	s-*si*	0.49 (2.67)	1.47 (1.50)	

[a] The graphic shows a schematic representation of the TSs corresponding to the attack of the *anti*/*syn*-enamine on the *re*/*si* face of the aldehyde (for catalyst **3**). [b] Gas-phase activation barriers $\Delta H^{\dagger}_{298\,K}$ including scaled zero-point energies obtained at the B3LYP/6-311+G**//B3LYP/6-31G* level are given in parentheses.

the lowest-energy TSs and the corresponding enantiomeric excess for all the proposed catalysts in this series are summarized in Table 1.

On the basis of the calculated absolute and relative activation barriers, it is noticed that the *syn*-enamines (s-*re*) derived from catalysts **1–7** tend to exhibit a general preference for *re*-face attack on the aldehyde. The TSs belonging to this series enjoy an additional C(β)H···O hydrogen bonding stabilization between the developing alkoxide and a suitably aligned C(β) hydrogen, as depicted in Fig. 1. The conformation of pyrrolidine in the bicyclic systems aids the formation of these favourable weak interactions, which could influence the relative stabilization of the diastereomeric TSs. As a rational design strategy, we envisaged that fine-tuning the acidity of C(β)H might have a direct bearing on the relative energies of the TSs. Thus, replacement of adjacent C(γ) methylene group of the azabicyclic system by more electronegative heteroatoms was considered. The presence of an α-heteroatom will impart enhanced acidity to the C(β) hydrogen and thus will

improve its ability towards stabilizing the developing alkoxide in the TS.[37] We have studied a series of α-heteroatom-substituted azabicyclic catalysts (**4** to **7**). Computed enantiomeric excesses with these catalysts are indeed found to be encouraging (Table 1). The enantiomeric excess is consistently higher than the corresponding unmodified bicyclic catalysts as well as the parent proline. For example, the predicted enantiomeric excess for catalyst **3** is 82%, while that for **5** is as high as 92%. These values are noticeably higher than the experimental values (as well as the DFT-predicted values) for the proline-catalyzed direct aldol reaction.[38]

The nature and position of the substituents on the catalyst could be employed as an effective method in fine-tuning the stereoselectivity. This is evident from the modest improvement in the enantiomeric excess noticed for catalyst **1** when compared to **2**. When the methyl substituent is placed closer to the enamine, as in **1**, the stereoselectivity is found to be better. Further elaborations using larger substituents could be valuable for improving the overall selectivity, even for sterically unbiased substrates. Examination of the optimized TS geometries provided in Fig. 1 clearly shows that the C(β′) substituent can directly influence the orientation of the carboxylic acid group, which in turn can affect the crucial proton transfer process. To confirm the existence of any such effects, the C(β′)H in a representative case (catalyst **4**) is substituted by a chlorine atom. As in the previously described approach, all four TSs for this modified catalyst are identified.

Geometric comparison between these catalysts can be performed with the help of the optimized geometries provided in Fig. 2. The orientation of the carboxylic acid group in the TSs when C(β′)-H is substituted with chlorine, labeled as **4′**, is found to be different from that in catalyst **4** ((a) and (b) in Fig. 2).[39] The computed enantiomeric excess for **4′** is found to be quite similar to that for the corresponding unsubstituted system (**4**). Another critical position on the catalyst framework is the C(β) position. In the lowest energy addition TSs for the [2.1.1] and [2.2.1] catalysts,

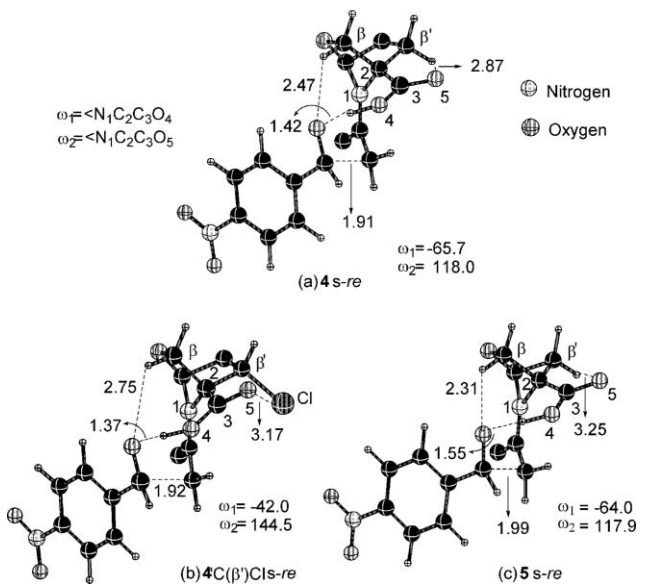

Fig. 2 The B3LYP/6-31G*-optimized lowest-energy TSs of catalysts **4** and **4′** (with Cl at the C(β′) position) and **5**. Only selected hydrogens on the catalyst are shown for clarity. Angles are given in degrees and distances in Å.

the C(β)H $\cdots$ $O^{\delta-}$ interaction is found to be stronger in the [2.1.1] catalyst, according to the optimized distances (Fig. 2a,c).[40] The effect of the C(β′)H $\cdots$ O=C–O interaction in influencing the carboxylic acid group orientation is found to be nearly nonexistent with the [2.1.1] system (a distance as large as 3.3 Å is noticed in the case of catalyst **5**). Interestingly, both these catalysts (**4** and **5**) are predicted to give nearly the same enantiomeric excess (Table 1). Therefore, the orientation of the carboxylic acid group does not seem to directly relate to the stereoselectivity, while the activation barriers are found to be different in catalysts **4** and **5**.

Computed activation barriers of the C–C bond formation step with the *syn*-enamine derived from [2.1.1] catalysts are found to be much lower than that with the [2.2.1] catalysts. Further, the energy differences between the TSs for *syn*- and *anti*-enamine additions to the electrophile are more pronounced in the [2.1.1] system. Inspection of the imaginary frequencies pertaining to the desired reaction coordinate convey interesting facts. While the imaginary frequency in the case of *anti*-enamines corresponds to the concomitant C–C bond formation and the proton transfer, it is dominated by the C–C bond formation in the case of the *syn*-enamines. On the basis of the C–C bond distances (in the range 1.95–2.10 Å with *syn*-enamines and 1.75–1.85 Å with *anti*-enamines)[41] and the proton transfer distances in the TSs, it is evident that the *syn*-enamines proceed through a relatively early transition state, whereas late transition states are noticed for the *anti*-enamines.

Another structurally different type of catalyst considered in this study has the C-β (C-7) of the pyrrolidine ring at the apical position in the [2.2.1] bicyclic system (**8**). The *syn*-enamine generated from catalyst **8** is found to be marginally more stable than the corresponding *anti*-enamine. Among the four stereochemical modes of addition of enamine to the electrophile, the a-*re* TS is the lowest energy TS leading to C–C bond formation (Fig. 3). Geometrical features provided additional insights on the factors contributing to the energy differences between these TSs.

A network of stabilizing weak interactions is found to be relatively in favour of the *anti*-enamine TSs. These include (i) a hydrogen bonding interaction between the developing alkoxide and the partially positive hydrogen of carbon adjacent to nitrogen (Fig. 3, $^{\delta+}$NC(α)H $\cdots$ $O^{\delta-}$ = 2.62 Å in a-*re*/a-*si*), (ii) intramolecular hydrogen bonding between C(β)H and the developing alkoxide (2.76 Å in a-*re* and 2.81 Å in a-*si*), and (iii) a Coulombic interaction between the incipient iminium nitrogen ($N^{\delta+}$) and the alkoxide (2.67 Å in a-*re* and 2.68 Å in a-*si*). In an effort to achieve optimal proton transfer distance between the carboxylic acid group and the developing alkoxide in *syn*-enamine TSs, change in orientation of the substituents around the incipient C–C bond takes place and results in lowering of intramolecular stabilizing interactions. The orientation of substituents around the forming C–C bond is more eclipsed in the *syn*-enamine TSs. The highest-eclipsing interactions are found with the s-*si* TS. (Fig. 3, $\omega = -118°$ in s-*si*) In all the TSs (derived both from *syn*-enamines and *anti*-enamines), the orientation of the carboxylic acid group is found to be assisted by an additional interaction between the -COOH group and C(β′)H (Fig. 3).

The computed activation barriers for the addition of *syn*-enamines derived from catalysts **8** are much higher than that for the corresponding *anti*-enamines. Now, among the two lower energy diastereomeric TSs from *anti*-enamines, the a-*re* TS is found to

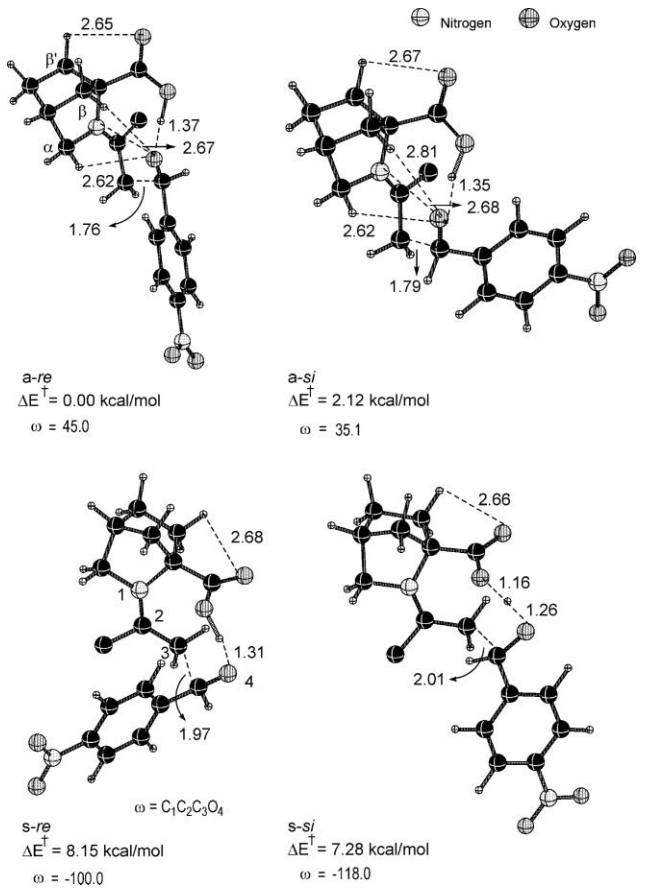

Fig. 3 The B3LYP/6-31G*-optimized transition state geometries for four unique stereochemical modes of addition for enamines derived from catalyst **8** to *p*-nitrobenzaldehyde. The key weak interactions contributing to the transition state stabilization are shown. Only selected hydrogens on the catalyst are shown for clarity. Activation barriers, $\Delta E^{\dagger}$, are obtained at the CPCM/B3LYP/6-311+G**//B3LYP/6-31G* level using DMSO as the solvent. Angles are given in degrees and distances in Å.

be the lowest energy TS, where the phenyl substituent is in the least-hindered position (Fig. 3). The energy difference between the two lower energy TSs (a-*re* and a-*si*) leading to diastereomeric products is found to be 2.12 kcal mol^{-1}, corresponding to an enantiomeric excess of 95%. Comparison of activation barriers and enantiomeric excesses for this series of catalysts (**8**, **9** and **10**) are grouped together in Table 2.

In another group of catalysts considered in the present study, the envelope conformer of the parent proline is maintained, as part of a bicyclic system, as in **9** and **10**. These catalysts also exhibited a preference towards *anti*-enamine addition involving the a-*re* TS as the lowest energy pathway. A more staggered arrangement of substituents around the new C–C bond is noticed with the *anti*-enamine TSs, while it is more eclipsed with the *syn*-enamine TSs.[35] Such geometric features evidently lead to a higher-energy TSs for the *syn*-enamine addition pathway. Between the *anti*-enamine TSs, the *re*-facial attack on the aldehyde is favoured over the corresponding *si*-facial approach, since the aryl substituent on the aldehyde in the former is found to be sterically better positioned.[42]

Perhaps the most striking feature emerging from the present investigation relates to the correlation between the catalyst structure and stereoselectivity. The agreement between the computed enantiomeric excess with that obtained experimentally for proline-catalyzed aldol reaction is found to be excellent. The ee predicted by DFT and the experimental value are 75% and 76% respectively.[3a,38] It is worthwhile to compare the enantiomeric excess calculated for catalysts **9** and **10** with that of proline, from a structure-selectivity point of view. The predicted ee for catalyst **9** is conspicuously quite close (74%) to the parent proline. In compounds **9** and **10**, even though the same proline conformation can be thought of as being constrained in a bicyclic framework, the increased rigidity of the [2.1.1] system is found to be good in improving the enantiomeric excess in **10** (Table 2).[43]

Table 2 Computed activation barriers $\Delta E^{\dagger}$ obtained at the CPCM$_{(DMSO)}$/B3LYP/6-311+G**//B3LYP/6-31G* level for the addition of enamines to *p*-nitrobenzaldehyde, and the corresponding enantiomeric excess for **8** to **11**

Catalysts	Mode of approach	$\Delta E^{\dagger}$/kcal mol^{-1} [a] Absolute	Relative	ee (%)
8	a-*re*	6.55 (4.56)	0.00 (0.00)	95 (95)
	a-*si*	8.68 (6.76)	2.12 (2.20)	
	s-*re*	15.34 (13.94)	8.15 (8.61)	
	s-*si*	14.47 (12.23)	7.28 (6.90)	
9	a-*re*	3.56(5.95)	0.00 (0.00)	75 (88)
	a-*si*	4.69 (7.62)	1.12 (1.66)	
	s-*re*	15.55 (13.03)	10.48 (2.77)	
	s-*si*	7.92(13.91)	2.86 (3.64)	
10	a-*re*	7.90 (6.74)	0.00 (0.00)	80 (91)
	a-*si*	9.21 (8.62)	1.31 (1.87)	
	s-*re*	5.67 (9.23)	1.19(2.02)	
	s-*si*	6.54 (10.06)	2.06 (2.84)	
11	a-*re*	7.87 (13.30)	3.62 (7.57)	5 (65.2)
	a-*si*	8.57 (12.88)	4.32 (7.16)	
	s-*re*	4.72 (5.95)	0.06 (0.00)	
	s-*si*	4.66 (6.88)	0.00 (0.92)	

[a] Gas-phase activation barriers $\Delta H^{\dagger}_{298\,K}$ including scaled zero-point energies computed at the B3LYP/6-311+G**//B3LYP/6-31G* level are given in parentheses.

The position, orientation and acidity of the carboxylic acid group are known to be important in contributing to the catalytic ability of proline and its derivatives in promoting aldol reactions. For instance, proline and pyrrolidine-3-carboxylic acid have been reported to yield products of opposite stereochemistry in the Mannich reaction between 3-pentanone and *N*-PMP-protected α-iminoester.[44] To verify how a bifunctional variant of proline (with a 1,3 relationship between the amino group and the carboxylic acid) performs compared to other bicyclic catalysts, we considered a [2.1.1] bicyclic system (Scheme 4, catalyst **11**). The computed activation barriers and the enantiomeric excess are given in Table 2. Though the carboxylic acid group is not adjacent to the enamine nitrogen, the distance is found to be close enough to facilitate the crucial proton transfer to the developing alkoxide.[45] In the case of catalyst **11**, the *syn*-enamine is found to be more stable than the *anti*-enamine. Further, the TSs resulting from the *syn*-enamines are much stable than those formed from the *anti*-enamines, but the energy difference between the *syn*-enamine TSs is very low. Hence the overall enantioselectivity of this catalyst is found to be the lowest among the present series of catalysts investigated. Based on the computed enantiomeric excess, it seems evident that the 1,2-relationship between the secondary amino group and the

carboxylic acid group is a highly desirable feature for amino acids to act as potential asymmetric catalysts for aldol reactions.

Encouraged by the enhanced stereoselectivity predicted for the bicyclic variants of proline, we have decided to examine how substrate-level changes (electrophilic aldehyde) will respond to these catalysts. Different substitutions on the aromatic aldehyde are therefore studied for their reaction with the enamine derived from a representative catalyst (**2**). Methyl substitution at the 2,6-positions of the aromatic aldehyde are found to be quite effective, increasing the enantiomeric excess up to 99%. Furthermore, the role of electronically active substituents (at the *para*-position) on the energetics of addition has also been investigated. The calculated activation barrier, as well as the enantiomeric excess, showed little variation compared to the original *p*-nitrobenzaldehyde.[46]

Conclusions

The possible role of azabicyclic compounds (**1–10**) as potential organocatalysts in asymmetric aldol reaction between acetone and *p*-nitrobenzaldehyde are investigated. The stereoselectivity-determining step, similar to that of the established proline-catalyzed aldol reactions, are carefully examined by locating all stereochemically pertinent transition states using DFT methods. The calculations showed that these catalysts could be highly effective for aldol reactions, compared to popular organocatalysts such as proline. The simplest bicyclic analogues of proline are predicted to give better enantiomeric excesses. Suitable substitutions on these bicyclic frameworks are found to be a superior protocol in modulating the stereoselectivity of bifunctional secondary amino acids. Catalysts **1–8**, which are predicted to give enantiomeric excess from 82 to 95%, are expected to be superior over proline, for which the calculated enantiomeric excess is only 75%. The reaction is expected to proceed with greater ease, as the predicted activation energies are lower. Analysis of various intramolecular interactions, such as Coulombic and hydrogen bonding interactions, operating in the diastereomeric transition states, are found to be helpful in rationalizing the predicted stereoselectivity induced by these catalysts.

Computational methods

Geometry optimization of reactants, intermediates, and transition states were carried out at the B3LYP/6-31G* level of theory[13,47] using the Gaussian 98 and Gaussian 03 suites of quantum chemical programs.[48] All the stationary points on the respective potential energy surfaces were characterized at the same level of theory by evaluating corresponding Hessian indices. Enthalpies were obtained by adding scaled zero-point vibrational energy corrections (ZPVE)[49] and thermal contributions to the gas-phase energies using standard statistical mechanics procedures as implemented in the Gaussian suite. Careful verification of the unique imaginary frequencies for the transition states has been carried out to check whether the frequency indeed pertains to the desired reaction coordinate. Further, intrinsic reaction coordinate (IRC) calculations were carried out to authenticate the transition states.[50,51] Activation barriers refer to the enthalpy of activation, obtained as the energy difference between isolated reactants and the corresponding transition state structures. Enthalpies are calculated by adding scaled ZPVE (0.9806)[49] and thermal contributions to the 'bottom-of-the-well' energy values. Single-point energies were then calculated using a more flexible triple zeta quality basis set, namely the 6-311+G** (with 6d-functions) with the continuum solvation model, using the SCRF-CPCM method,[52] with the united-atom Kohn–Sham (UAKS) radii. DMSO was used as the continuum solvent dielectric (ε = 46.7). All the SCRF calculations were performed with the default options implemented in Gaussian 03. These energy values include the solvent polarity effects, in the form of electrostatic terms, on the gas-phase-computed energies. Earlier reports have suggested that the electrostatic contributions are more important than the non-electrostatic terms in the continuum models.[53] The estimates based on these values are also found to be in very good agreement with the experimentally available selectivity known for proline.[38] Unless otherwise specified, the values reported within the SCRF-CPCM framework pertains to the free energy of solvation G^{el}_{sol} with all the electrostatic terms (denoted as E in the text). Full geometry optimizations with the continuum solvation model might lead to changes in geometries and energetics. Unfortunately, such calculations are prohibitively expensive on larger molecules (with regard to the level of theory) reported here. Further, the focus is on the relative energies of diastereomeric transition states than on the absolute activation parameters. One can therefore expect that the computed values should be sufficiently reliable to be able to draw meaningful conclusions.

Acknowledgements

We are grateful to the Department of Science and Technology, New Delhi, for financial support (through SR/S1/OC-50/2003), and the IITB computer center for computing facilities. SCB acknowledges CSIR New Delhi for a Junior Research Fellowship.

References and notes

1 (*a*) G. Zhong, T. Hoffmann, R. A. Lerner, S. Danishefsky and C. F. Barbas, III, *J. Am. Chem. Soc.*, 1997, **119**, 8131; (*b*) G. Zhong, R. A. Lerner and C. F. Barbas, III, *Angew. Chem., Int. Ed.*, 1999, **38**, 3738; (*c*) P. I. Dalko and L. Moisan, *Angew. Chem., Int. Ed.*, 2001, **40**, 3726; (*d*) P. R. Schreiner, *Chem. Soc. Rev.*, 2003, **32**, 289; (*e*) P. I. Dalko and L. Moisan, *Angew. Chem., Int. Ed.*, 2004, **43**, 5138; (*f*) J. Seayad and B. List, *Org. Biomol. Chem.*, 2005, **3**, 719; (*g*) B. List and J. W. Yang, *Science*, 2006, **313**, 1584; (*h*) B. List, *Acc. Chem. Res.*, 2004, **37**, 548; (*i*) F. Cozzi, *Adv. Synth. Catal.*, 2006, **348**, 1367.

2 (*a*) B. List, *Tetrahedron*, 2002, **58**, 5573; (*b*) M. Movassaghi and E. N. Jacobsen, *Science*, 2002, **298**, 1904; (*c*) A. B. Northrup and D. W. C. MacMillan, *J. Am. Chem. Soc.*, 2002, **124**, 6798; (*d*) A. B. Northrup, I. K. Mangion, F. Hettche and D. W. C. MacMillan, *Angew. Chem., Int. Ed.*, 2004, **43**, 2152; (*e*) M. Marigo, S. Bachmann, N. Halland, A. Braunton and K. A. Jorgenson, *Angew. Chem., Int. Ed.*, 2004, **43**, 5507.

3 (*a*) K. Saktivel, W. Notz, T. Bui and C. F. Barbas, III, *J. Am. Chem. Soc.*, 2001, **123**, 5260; (*b*) E. R. Jarvo and S. J. Miller, *Tetrahedron*, 2002, **58**, 2481; (*c*) W. Notz, F. Tanaka and C. F. Barbas, III, *Acc. Chem. Res.*, 2004, **37**, 580; (*d*) E. Bellis and G. Kokotos, *Tetrahedron*, 2005, **61**, 8669; (*e*) Z. Tang, Z.-H. Yang, X.-H. Chen, L.-F. Cun, A.-Q. Mi, Y.-Z. Jiang and L.-Z. Gong, *J. Am. Chem. Soc.*, 2005, **127**, 9285; (*f*) J.-R. Chen, H.-H. Lu, X.-Y. Li, L. Cheng, J. Wan and W.-J. Xiao, *Org. Lett.*, 2005, **7**, 4543; (*g*) N. Halland, M. A. Lie, A. Kjærsgaard, M. Marigo, B. Schiott and K. A. Jorgenson, *Chem.–Eur. J.*, 2005, **11**, 7083; (*h*) C. Cheng, C. Sun, C. Wang, Y. Zhang, S. Wei, F. Jiang and Y. Wu, *Chem. Commun.*, 2006, 215; (*i*) L. Gu, M. Yu, X. Wu, Y. Zhang and G. Zhao, *Adv. Synth. Catal.*, 2006, **348**, 2223.

4 (*a*) Z. Tang, F. Jiang, L. Yu, X. Cui, L. Gong, A. Mi, Y. Jiang and Y. Wu, *J. Am. Chem. Soc.*, 2003, **125**, 5262; (*b*) K. N. Houk and P. H.-Y. Cheong, *Synthesis*, 2005, **9**, 1533.

5 (*a*) B. List, P. Pojarliev, W. T. Biller and J. M. Martin, *J. Am. Chem. Soc.*, 2002, **124**, 827; (*b*) S. Bahmanyar and K. N. Houk, *Org. Lett.*, 2003, **5**, 1249; (*c*) S. P. Brown, M. P. Brochu, C. J. Sinz and D. W. C. MacMillan, *J. Am. Chem. Soc.*, 2003, **125**, 10808; (*d*) N. Vignola and B. List, *J. Am. Chem. Soc.*, 2004, **126**, 450; (*e*) A. Fu, B. List and W. Thiel, *J. Org. Chem.*, 2006, **71**, 320.
6 Z. G. Hajos and D. R. Parrish, *J. Org. Chem.*, 1974, **39**, 1615.
7 (*a*) C. Agami, C. Puchot and J. Levisalles, *J. Chem. Soc., Chem. Commun.*, 1985, **441**; (*b*) C. Puchot, O. Samuel, E. Dunach, S. Zhao, C. Agami and H. B. Kagan, *J. Am. Chem. Soc.*, 1986, **108**, 2353.
8 S. Bahmanyar and K. N. Houk, *J. Am. Chem. Soc.*, 2001, **123**, 12911.
9 F. R. Clemente and K. N. Houk, *J. Am. Chem. Soc.*, 2005, **127**, 11294.
10 M. E. Jung, *Tetrahedron*, 1976, **32**, 3.
11 L. Hoang, S. Bahmanyar, K. N. Houk and B. List, *J. Am. Chem. Soc.*, 2003, **125**, 16.
12 (*a*) P. H.-Y. Cheong and K. N. Houk, *J. Am. Chem. Soc.*, 2004, **126**, 13912; (*b*) P. H.-Y. Cheong, H. Zhang, R. Thayumanavan, F. Tanaka, K. N. Houk and C. F. Barbas, III, *Org. Lett.*, 2006, **8**, 811.
13 (*a*) A. D. Becke, *J. Chem. Phys.*, 1993, **98**, 5648; (*b*) A. D. Becke, *Phys. Rev. A*, 1998, **38**, 3098; (*c*) C. Lee, W. Yang and R. G. Parr, *Phys. Rev. B*, 1998, **37**, 785.
14 (*a*) A. Córdova, *Angew. Chem., Int. Ed.*, 2005, **44**, 7028; (*b*) J. Joseph, D. B. Ramachary and E. D. Jemmis, *Org. Biomol. Chem.*, 2006, **4**, 2685.
15 (*a*) L. Hoang, S. Bahmanyar, K. N. Houk, H. J. Martin and B. List, *J. Am. Chem. Soc.*, 2003, **125**, 2475; (*b*) C. Allemann, R. Gordillo, F. R. Clemente, K. N. Houk and P. H.-Y. Cheong, *Acc. Chem. Res.*, 2004, **37**, 558.
16 M. S. Taylor and E. N. Jacobsen, *Angew. Chem., Int. Ed.*, 2006, **45**, 1520.
17 (*a*) K. N. Rankin, J. W. Gauld and R. J. Boyd, *J. Phys. Chem. A*, 2002, **106**, 5155; (*b*) L. R. Domingo and M. Arnó, *Theor. Chem. Acc.*, 2002, **108**, 232.
18 F. R. Clemente and K. N. Houk, *Angew. Chem., Int. Ed.*, 2004, **43**, 5766.
19 Gas phase activation enthalpies ($\Delta H_{298\,K}$) have earlier been established to have smallest errors (when compared with experimentally determined activation parameters as well as enantioselectivities) for the proline-catalyzed asymmetric intermolecular aldol reaction between acetone or cyclohexanone with a number of electrophiles such as benzaldehyde, isobutyraldehyde and so on. See ref. 15*a*.
20 (*a*) G. Ujaque, F. Maseras and A. Lledós, *J. Am. Chem. Soc.*, 1999, **121**, 1317; (*b*) J. Vázquez, M. A. Pericas, F. Maseras and A. Lledós, *J. Org. Chem.*, 2000, **65**, 7303; (*c*) D. Balcells, F. Maseras and G. Ujaque, *J. Am. Chem. Soc.*, 2005, **127**, 3624.
21 (*a*) B. A. Grzybowski, A. V. Ishchenko, J. Shimada and E. I. Shakhnovich, *Acc. Chem. Res.*, 2002, **35**, 261; (*b*) H. M. Howard, T. Cenizal, S. Gutteridge, W. S. Hanna, Y. Tao, M. Totrov, V. A. Wittenbach and Y.-J. Zheng, *J. Med. Chem.*, 2004, **47**, 6669; (*c*) M. C. Kozlowski, S. P. Waters, J. W. Skudlarek and C. A. Evans, *Org. Lett.*, 2002, **4**, 4391; (*d*) M. Panda, M. C. Kozlowski and P.-W. Phuan, *J. Org. Chem.*, 2003, **68**, 564.
22 (*a*) J. A. Cobb, D. M. Shaw, D. A. Longbottom, J. B. Gold and S. V. Ley, *Org. Biomol. Chem.*, 2005, **3**, 84; (*b*) Y. Hayashi, T. Sumiya, J. Takahashi, H. Gotoh, T. Urushima and M. Shoji, *Angew. Chem., Int. Ed.*, 2006, **45**, 958; (*c*) L. Zu, J. Wang, H. Li and W. Wang, *Org. Lett.*, 2006, **8**, 3077; (*d*) S. Luo, X. Mi, L. Zhang, S. Liu, H. Xu and J.-P. Cheng, *Angew. Chem., Int. Ed.*, 2006, **45**, 3093.
23 For a report on 4,5-methanoprolines, see: K. N. Houk, J. S. Warrier, S. Hanessian and P. H.-Y. Cheong, *Adv. Synth. Catal.*, 2004, **346**, 1111.
24 (*a*) A. Córdova, W. Zou, I. Ibrahem, E. Reyes, M. Engqvist and W. Liao, *Chem. Commun.*, 2005, 3586; (*b*) A. Córdova, W. Zou, P. Dziedzic, I. Ibrahem, E. Reyes and Y. Xu, *Chem.–Eur. J.*, 2006, **12**, 5383.
25 E. Czinki and A. G. Császár, *Chem.–Eur. J.*, 2003, **9**, 1008.
26 (*a*) J. K. M. Sanders, *Chem.–Eur. J.*, 1998, **4**, 1378; (*b*) A. Wittikopp and P. R. Schreiner, *Chem.–Eur. J.*, 2003, **9**, 407.
27 See Table S4† on the synthetic availability or other applications of some of these proposed molecules.
28 J. Gante, *Angew. Chem., Int. Ed. Engl.*, 1994, **33**, 1699.
29 S. F. Nelson, J. T. Ippoliti, T. B. Frigo and P. A. Petillo, *J. Am. Chem. Soc.*, 1989, **111**, 1776.
30 C. Aleman, A. I. Jimenez, C. Cativiela, J. J. Perez and J. Casanovas, *J. Phys. Chem. B*, 2005, **109**, 11836.
31 Interestingly, such a restricted pyrrolidine conformation has been found as part of the natural product epibatidine. See: T. F. Spande, H. M. Garraffo, M. W. Edwards, L. Panel and J. W. Daly, *J. Am. Chem. Soc.*, 1992, **114**, 3475.
32 See Table S5† for the relative energies of the *syn*- and *anti*-enamines formed between acetone and catalysts **1–11**.
33 Similar geometric features for TSs in proline-catalyzed aldol reactions have been noticed previously. See ref. 8,15*a*.
34 The planarity of enamines have been studied in detail using X-ray crystallographic techniques; see: K. L. Brown, L. Damm, J. D. Dunitz, A. Eschenmoser, R. Hobi and C. Kratky, *Helv. Chim. Acta*, 1978, **61**, 3108.
35 A full list of C_{ring}–N–C–Ci_{minium} dihedral angles (given in Fig. 1 as θ_1–θ_4) are provided in Table S3†.
36 Hybrid Hartree–Fock DFT methods such as B3LYP can lead to systematic errors in estimating C–H $\cdots$ π interactions. We have therefore carried out additional single-point energy calculations using the *ab initio* MP2 method. Interestingly, the enantiomeric excess calculated based on the energies obtained at the MP2/6-311G**//B3LYP/6-31G*level for a representative catalyst **1** (85%) is found to be in good agreement with the ee calculated at the $CPCM_{(DMSO)}$/B3LYP/6-311+G**//B3LYP/6-31G* level (87%). While inclusion of higher-order electron correlation might result in changes in the predicted enantiomeric excess, the trends are likely to remain the same across the range of catalysts proposed here. Considering the size of the catalyst–substrate complex, these calculations would be prohibitively expensive.
37 This is reminiscent of the α-effect proposed in Diels–Alder reactions catalyzed by iminium ions; see: N. C. O. Tomkinson, J. L. Cavill and J. Peters, *Chem. Commun.*, 2003, 728.
38 The enantiomeric excess calculated based on the energies obtained at the $CPCM_{(DMSO)}$/B3LYP/6-311+G**//B3LYP/6-31G* level for the proline-catalyzed aldol reaction between acetone and *p*-nitrobenzaldehyde is given in Table S8†.
39 (*a*) A difference in dihedral angle value of 25° for the carboxylic acid orientation (ω_2) is noticed between unsubstituted and substituted cases; (*b*) the ee calculated for the **4**′C(β′)Cl-catalyzed aldol reaction is 90%.
40 The C(β)H $\cdots$ $O^{\delta-}{}_{alkoxide}$ distance in the s-*re* TS geometry for catalyst **5** (Fig. 2c) is 2.31 Å, whereas the corresponding distance in catalyst **4** is 2.47 Å (Fig. 2a).
41 For a complete description of transition state structural parameters for all the catalysts, see Table S1 and S2†.
42 See Fig. S3†.
43 See Fig. S4† for optimized geometries of the lowest energy TSs for catalyst **10**.
44 (*a*) H. Zhang, M. Mifsud, F. Tanaka and C. F. Barbas, III, *J. Am. Chem. Soc.*, 2006, **128**, 9630; (*b*) S. Mitsumori, H. Zhang, P. H.-Y. Cheong, K. N. Houk, F. Tanaka and C. F. Barbas, III, *J. Am. Chem. Soc.*, 2006, **128**, 1040.
45 Depending on how the enamine double bond is positioned with respect to the carboxylic acid group (nearer or farther away), it is termed as a *syn*-enamine and *anti*-enamine, respectively. See Fig. S5†.
46 (*a*) Calculated activation barriers and enantiomeric excesses are summarized in Table S6 and S7†; (*b*) Please see Fig. S2† for the optimized geometries of the lowest energy TSs for the aldol reaction between acetone and 2,6-dimethyl-4-nitrobenzaldehyde catalyzed by **2**.
47 (*a*) R. Ditchfield, W. J. Hehre and J. A. Pople, *J. Chem. Phys.*, 1971, **54**, 724; (*b*) W. J. Hehre, R. Ditchfield and J. A. Pople, *J. Chem. Phys.*, 1972, **56**, 2257; (*c*) P. C. Hariharan and J. A. Pople, *Theor. Chim. Acta*, 1973, **28**, 213.
48 (*a*) M. J. Frisch, *Gaussian 98 (Revision A.11.4)*, Gaussian, Inc., Pittsburgh, PA, 2002; (*b*) M. J. Frisch, *Gaussian 03 (Revision C.02)*, Gaussian, Inc., Wallingford, CT, 2004. See the ESI† for the full citation.
49 A. P. Scott and L. Radom, *J. Phys. Chem.*, 1996, **100**, 16502.
50 (*a*) C. Gonzalez and H. B. Schlegel, *J. Chem. Phys.*, 1989, **90**, 2154; (*b*) C. Gonzalez and H. B. Schlegel, *J. Phys. Chem.*, 1990, **94**, 5523.
51 See Table S9† for the IRC profiles for the lowest energy transition states of catalysts **1–11**.
52 (*a*) M. Cossi, V. Barone, R. Cammi and J. Tomasi, *J. Chem. Phys. Lett.*, 1996, **255**, 327; (*b*) E. Cancès, B. Mennucci and J. Tomasi, *J. Chem. Phys.*, 1997, **107**, 3032.
53 (*a*) D. W. Tondo and J. R. Pliego, Jr., *J. Phys. Chem. A*, 2005, **109**, 507; (*b*) G. Alagona, C. Ghio and S. Monti, *Phys. Chem. Chem. Phys.*, 2002, **2**, 4884.

